

# A spectral approach to 3-D object scattering in layered media applied to scattering from submerged spheres

Nicholas C. Makris

Massachusetts Institute of Technology, Cambridge, Massachusetts 02139

(Received 25 November 1997; revised 5 June 1998; accepted 16 June 1998)

A spectral formulation for 3-D object scattering in a layered medium is described. The formulation is valid when the source and receiver are sufficiently far from the object that multiple scattering between the object and waveguide boundaries can be neglected and the scattered field can be expressed as a linear function of the object's plane wave scattering function. An analytic expression is then derived for the field scattered from a spherical object in a stratified medium. Since the expression is in terms of 1-D wave number integrals, it is computationally efficient to implement, allows detailed investigation of the scattered field in the vicinity of the object, and enables scattering of evanescent waves to be incorporated by analytic continuation. Computations for a noncompact sphere ( $1 < ka$ ) illustrate the essential characteristics of 3-D object scattering in a shallow but multi-modal waveguide. Relative to free-space scattering, a significant decrease in the level of the scattered field in the forward direction as well as a pronounced directional beaming effect in the vicinity of the sphere are discovered. Another primary finding is that multistatic observations of the scattered field, distributed over an azimuthal aperture greatly in excess of  $\pi/(ka)$ , will typically be necessary to classify an object submerged in a shallow-water waveguide at ranges exceeding the water column depth. © 1998 Acoustical Society of America. [S0001-4966(98)01010-8]

PACS numbers: 43.30.Dr, 43.30.Gv, 43.30.Bp [SAC-B]

## INTRODUCTION

The purpose of this paper is to elucidate some essential characteristics of 3-D scattering by potentially noncompact ( $1 < ka$ ) objects in a shallow-water waveguide. To simplify matters, it is assumed that the source and receiver are sufficiently far from the object that multiple scattering between the object and waveguide boundaries can be neglected and the scattered field can be expressed as a linear function of the object's plane wave scattering function. These assumptions are in keeping with both Ingenito's modal formulation<sup>1</sup> and the more recent spectral approach of Makris *et al.* for scattering from an object in a layered medium.<sup>2</sup> The latter is adopted in the present paper because accurate solutions can be obtained for source and receiver locations that are much closer to the object than in the former discrete modal formulation. This makes way for a detailed investigation into the 3-D structure of the scattered field from relatively close proximity to the submerged object out to horizontal ranges in great excess of the water column depth.

Primary attention is given to the important special case of scattering from a sphere in a layered medium. While the sphere shares many basic 3-D scattering characteristics with other objects, it also has a solution that is practical to implement. For example, separation of variables is fully exploited to analytically express the field scattered from a sphere in a layered medium in terms of 1-D wave number integrals. The resulting expression is evaluated numerically to delineate some fundamental characteristics of noncompact object scattering in a shallow-water waveguide.

The spatial structure of the scattered field is then computed as a function of range, depth, and azimuth so near to a noncompact sphere that a directional beaming effect, apparently peculiar to objects submerged in a shallow but multi-

modal waveguide, is discovered. A significant reduction in the relative level of the scattered field in the forward direction, over what would be expected in free space, is also discovered. The spatial structure of the scattered field at horizontal ranges greatly in excess of the water column depth is then analyzed. Implications for the remote classification of general noncompact objects in a shallow waveguide are discussed. Additionally, estimates of the scattered field intensity obtained by standard, but crude, target strength, and sonar-equation analysis are found to be in drastic error. The present formulation for a sphere, therefore, is expected to be especially useful in many canonical shallow-water active detection and estimation problems. For example, the solution has already been used in simulating the coherent localization of humpback whales<sup>3</sup> and other submerged objects whose scattered fields are buried in surface-generated noise.<sup>4</sup>

The problem of scattering from a 3-D object in a stratified medium has been treated by a number of authors.<sup>1-11</sup> Ingenito notes<sup>1</sup> that work prior to his 1987 paper focuses on adapting the T-matrix method to the waveguide problem. The most comprehensive work of this period is that of Hackman and Sammelmann,<sup>6</sup> who developed a modal solution that includes the effect of multiple scattering between object and waveguide boundaries, but which requires use of the *free-field* Green function and is restricted to media with constant sound speed layers. As Hackman and Sammelmann later note,<sup>7</sup> Ingenito's use of the *waveguide* Green function greatly simplifies the problem when *multiple scattering* between the *object* and waveguide boundaries can be neglected. Moreover, Ingenito's *single-scatter* model<sup>1</sup> fully accounts for waveguide propagation effects, such as multiple reflections of the scattered field between waveguide boundaries, because it is based upon the *waveguide* Green function.

As a result, multiple images of the object will appear at the receiver. However, there will be no rescattering between these multiple images in the single-scatter model because it employs the *free-space* scatter function for the object. The single-scatter approximation is typically valid when the object is not too close to the waveguide boundaries, relative to its scale and the wavelength,<sup>1,2,6-11</sup> and so is useful in many practical scenarios.

The spectral formulation adopted here generalizes Ingenito's single-scatter model. It was originally introduced to investigate the plausibility of detecting and localizing submerged objects by their perturbation of an ocean waveguide's ambient noise field.<sup>2</sup> It has not been previously applied to the standard 3-D object-scattering problem where the source is restricted to an isolated point in the waveguide. The primary advantage of the spectral approach is that it enables the scattered field to be computed much closer to the object than in previous modal formulations.<sup>1,6,7,9-11</sup> Moreover, it has an extremely compelling physical interpretation. Specifically, the source and receiver are assumed to be sufficiently far from the object that its free-space scattering function can be used to linearize the problem, as implied in Ingenito's original modal formulation.<sup>1</sup> The field emanating from the source is then decomposed into plane waves incident on the object. The object scatters each incident plane wave into all directions by its free-space scattering function. The scattered field from each incident plane wave then propagates through the waveguide to the receiver in accord with the waveguide Green function. The scattered fields from each incident plane wave are coherently superposed to form the total scattered field at the receiver. Just as the great practical advantage of Ingenito's modal approach is its ease of implementation by straightforward modification of existing normal-mode propagation software,<sup>1</sup> the spectral generalization is advantageous because it can be easily implemented by straightforward modification of existing wave number integration software. Like the modal approach, the spectral formulation can be used to compute the scattered field from an *arbitrarily shaped penetrable object* as long as its free-space scattering function is known either analytically, as is the case for many simple shapes,<sup>12</sup> or experimentally, as in submarine target scattering.<sup>13</sup> For example, Perkins, Kuperman, Tinker, Heaney, and Murphy have employed Ingenito's modal approach to treat the problem of scattering from a prolate spheroid in a deep ocean waveguide.<sup>9,10</sup> While the spectral approach described here is for a harmonic source, it is readily extended to the time domain by standard Fourier synthesis.

In related work, Collins and Werby<sup>8</sup> describe a parabolic equation (PE) method for 3-D object scattering in the ocean. The advantage of this approach is its ability to handle range-dependent waveguides. A primary disadvantage is that the 3-D PE must generally be used to properly handle diffraction about the object so that the entire 3-D field from the object must be marched to the range of the receiver even if the receiver is isolated at a single point in range, depth, and azimuth. Additionally, Perkins *et al.*<sup>9,10</sup> have used the adiabatic approximation to extend Ingenito's modal approach for 3-D object scattering to weakly range-dependent

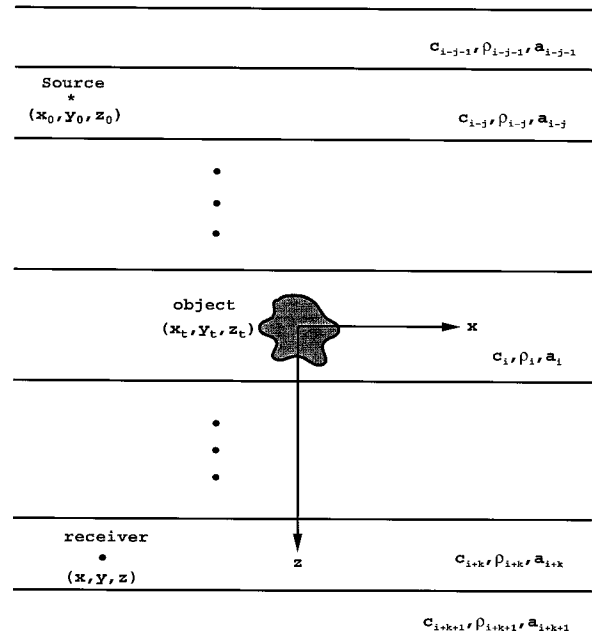


FIG. 1. Geometry of an object, source and receiver in a horizontally stratified medium. All coordinate systems are centered at the object centroid. Each layer  $i$  is characterized by sound speed  $c_i$ , density  $\rho_i$ , and attenuation  $a_i$ .

waveguides. As in the original modal formulation, this extension is only valid when the range from the source, and receiver, to the object is much greater than the waveguide depth.

For economy, the notation of Ref. 2 is used here and in the remainder of this article. For example, the object centroid is at the center of all coordinate systems, as shown in Fig 1. Source coordinates are defined by  $(x_0, y_0, z_0)$ , receiver coordinates by  $(x, y, z)$  and coordinates on the surface of the object by  $(x_i, y_i, z_i)$  where the positive  $z$  axis points downward and normal to the interfaces between horizontal strata. Spatial cylindrical  $(\rho, \theta, z)$  and spherical systems  $(r, \theta, \phi)$  are defined by  $x = r \sin \theta \cos \phi$ ,  $y = r \sin \theta \sin \phi$ ,  $z = r \cos \theta$ , and  $\rho^2 = x^2 + y^2$ . Wave number coordinates for the incident  $(\xi_{ix}, \xi_{iy}, \gamma_i)$  and scattered field  $(\xi_x, \xi_y, \gamma)$  are related to polar and azimuthal propagation angles  $(\alpha, \beta)$  by  $\xi_x = k \sin \alpha \cos \beta$ ,  $\xi_y = k \sin \alpha \sin \beta$ ,  $\gamma = k \cos \alpha$ , where the horizontal wave number magnitude is defined by  $\xi^2 = \xi_x^2 + \xi_y^2$  and the wave number magnitude  $k$  equals the angular frequency  $\omega$  divided by the sound speed  $c$ . For example, the phase  $\mathbf{k} \cdot \mathbf{r}$  is explicitly written as

$$\xi \cdot \boldsymbol{\rho} + \gamma z = kr [\cos \alpha \cos \theta + \sin \alpha \sin \theta \cos(\beta - \phi)]. \quad (1)$$

## I. AN APPROXIMATION FOR 3-D SCATTERING FROM AN OBJECT OF ARBITRARY SHAPE IN A LAYERED MEDIUM

The harmonic field  $\Phi_s(\mathbf{r})$  scattered by an object can be expressed in terms of the medium Green function  $G(\mathbf{r}|\mathbf{r}_t)$  and incident field  $\Phi_i(\mathbf{r})$  by Kirchoff's integral equation

$$\Phi_s(\mathbf{r}) = - \int_{A_t} \int [\Phi_i(\mathbf{r}_t) + \Phi_s(\mathbf{r}_t)] \frac{\partial G(\mathbf{r}|\mathbf{r}_t)}{\partial n_t} + G(\mathbf{r}|\mathbf{r}_t) \frac{\partial}{\partial n_t} [\Phi_i(\mathbf{r}_t) + \Phi_s(\mathbf{r}_t)] dA_t, \quad (2)$$

where  $G(\mathbf{r}|\mathbf{r}_t)$  and  $\Phi_i(\mathbf{r})$  each satisfy the Helmholtz equation, driven by a point source of unit strength at angular frequency  $\omega$ .

In many practical applications, however, a number of simplifying assumptions can be made that lead to an approximate formulation that is both intuitively appealing and far less computationally expensive to solve than Kirchhoff's integral equation. This approximation is valid when: (1) the propagation medium is horizontally stratified and range independent; (2) the object is contained within a layer whose index of refraction can be well approximated as a constant; (3) multiple reflections between the *object* and waveguide boundaries make a negligible contribution to the scattered field at the location of a receiver; and (4) the range from the object to the source, and receiver, is large enough that the scattered field can be expressed as a linear function of the object's plane wave scatter function. This last assumption often requires that the range from the object is much greater than the object's spatial extent.

While the field scattered from an object in a horizontally stratified medium can always be expressed in terms of a 4-D horizontal wave number transform, this approach becomes particularly useful when the conditions listed above are satisfied. Then the kernel of the spectral transform can be approximated as a function that is independent of the horizontal positions of the source, potentially noncompact scatterer and receiver. In this case, Makris *et al.*<sup>2</sup> show that the scattered field becomes

$$\Phi_s(\mathbf{r}) = \frac{1}{\pi k} \int \int_{-\infty}^{\infty} F(z, z_0, \xi, \xi_i) e^{i(\xi_i \cdot \rho_0 + \xi \cdot \rho)} d^2 \xi_i d^2 \xi, \quad (3)$$

where the kernel,

$$\begin{aligned} F(z, z_0, \xi, \xi_i) \approx & \Psi^+(z_0) \Psi^+(z) S(\pi - \alpha, \beta; \pi - \alpha_i, \beta_i) \\ & + \Psi^+(z_0) \Psi^-(z) S(\alpha, \beta; \pi - \alpha_i, \beta_i) \\ & + \Psi^-(z_0) \Psi^+(z) S(\pi - \alpha, \beta; \alpha_i, \beta_i) \\ & + \Psi^-(z_0) \Psi^-(z) S(\alpha, \beta; \alpha_i, \beta_i), \end{aligned} \quad (4)$$

is a function of the object's plane wave scattering function in free space  $S(\alpha, \beta; \alpha_i, \beta_i)$ ,<sup>12</sup> and down-going (positive superscript) and up-going (negative superscript) plane wave amplitudes  $\Psi^+(z_0)$ ,  $\Psi^-(z_0)$ ,  $\Psi^+(z)$ , and  $\Psi^-(z)$ . These plane wave amplitudes depend explicitly on the depth of the source or receiver, and implicitly on the depth of the object's centroid because the centroid is chosen to be at the origin of the coordinate system. By spectral transformation, these amplitudes can be used to express the incident field

$$\Phi_i(\mathbf{r}_t|\mathbf{r}_0) = \frac{1}{2\pi} \int_{-\infty}^{\infty} \{ \Psi^+(z_0) e^{i\gamma z_t} + \Psi^-(z_0) e^{-i\gamma z_t} \} \times e^{-i\xi_i \cdot (\rho_t - \rho_0)} d^2 \xi_i, \quad (5)$$

and waveguide Green function

$$G(\mathbf{r}|\mathbf{r}_t) = \frac{1}{2\pi} \int_{-\infty}^{\infty} \{ \Psi^+(z) e^{i\gamma z_t} + \Psi^-(z) e^{-i\gamma z_t} \} \times e^{i\xi \cdot (\rho - \rho_t)} d^2 \xi, \quad (6)$$

in terms of up and down going plane waves. In the former expression, the plane wave amplitudes relate transmission from the layer of the point source to a receiver in the layer of the object. In the latter they relate transmission from the layer of the object to that of the receiver. They also depend, therefore, on the magnitude of the horizontal wave number and the boundary conditions at the interfaces between the layers.

Equations (3)–(4) reveal a simple prescription for computing the field scattered from an object in a layered medium where preliminary propagation and scattering computations are made independently. For example, to set up the propagation component of the calculation, the up- and down-going plane wave amplitudes are computed just as they are for point–source to point–receiver propagation in a range-independent horizontally stratified media. Any of a number of standard techniques can be used for this purpose.<sup>14,15</sup> For the scattering component, the object's plane wave scattering function in free space may either be already known, as is the case for many simple shapes;<sup>12</sup> it may be experimentally measured, as for example in submarine target scattering;<sup>13</sup> or it may be computed by standard asymptotic methods.<sup>12</sup> The results of this preliminary analysis are then incorporated in Eqs. (3)–(4) and the scattered field is computed by wave number integration.

Equations (3)–(4) are also intuitively appealing. The incident field is decomposed into a continuum of up- and down-going plane waves in accord with propagation in a horizontally stratified waveguide, or specifically Eq. (5). Any one of these incident plane waves is scattered from the object into a continuum of directions. This continuum of scattered plane waves is then organized into an up-going and a down-going set, as required by the waveguide Green function in Eq. (6). When the approximation is valid, the total scattered field is then just the integral of all plane wave components scattered from every incident plane wave component.

## II. SCATTERING FROM A SPHERICAL OBJECT IN A LAYERED MEDIUM

To derive an expression for the field scattered from a spherical object in a layered medium, Eq. (3) is first rewritten as

$$\Phi_s(\mathbf{r}) = \frac{1}{\pi k} \int_0^{\infty} \xi d\xi \int_0^{\infty} \xi_i d\xi_i \int_0^{2\pi} d\beta \int_0^{2\pi} d\beta_i \times F(z, z_0, \xi, \xi_i) e^{i(\rho_i \cdot \xi_0 + \rho \cdot \xi)}, \quad (7)$$

where each 2-D integral is expressed in terms of polar coordinates over the magnitude and direction of the respective horizontal wave number vector. As a consequence of the spherical symmetry of the object, a number of simplifications can be made. To this end, the plane wave scattering function for a spherical object is introduced.

As shown in Appendix A of Ref. 2, the addition theorem for spherical harmonics can be used to express the plane wave scattering function for a sphere in free space as

$$S(\alpha, \beta; \alpha_i, \beta_i) = \sum_{n=0}^{\infty} f(n) \left\{ P_n \left( \frac{\gamma}{k} \right) P_n \left( \frac{\gamma_i}{k} \right) + 2 \sum_{m=1}^n \frac{(n-m)!}{(n+m)!} \right. \\ \left. \times P_n^m \left( \frac{\gamma}{k} \right) P_n^m \left( \frac{\gamma_i}{k} \right) \cos m(\beta - \beta_i) \right\}, \quad (8)$$

where

$$f(n) = i(-1)^n (2n+1) a_n, \quad (9)$$

and the coefficient

$$a_n = \frac{j'_n(ka) - (\rho c / \rho_t c_t) [j'_n(k_t a) / j_n(k_t a)] j_n(ka)}{h'_n(ka) - (\rho c / \rho_t c_t) [j'_n(k_t a) / j_n(k_t a)] h_n(ka)}, \quad (10)$$

is determined by boundary conditions at the sphere's surface given internal density  $\rho_t$ , sound speed  $c_t$ , and wave number  $k_t = \omega / c_t$ .<sup>16</sup> Equation (8) is convenient for two reasons. First, it factors the polar wave number components in such a way that they can be easily integrated out. Second, it expresses the vertical directionality of the incident and scattered waves

in terms of the vertical wave number magnitudes. These attributes are essential for the scattered field to be expressed exclusively in terms of integrals over the horizontal wave number magnitudes. They also enable evanescent waves to be incorporated by analytic continuation to horizontal wave number magnitudes beyond  $k$ , which corresponds to imaginary incident and scattered angles.

After substituting this scattering function in Eqs. (4) and (7), integrals over the horizontal wave number's polar angle are carried out with the aid of the easily proven identities

$$\int_0^{2\pi} d\beta \int_0^{2\pi} d\beta_i e^{i\{\xi_i \rho_0 \cos(\beta_i - \phi_0) + \xi \rho \cos(\beta - \phi)\}} \\ = (2\pi)^2 J_0(\xi_i \rho_0) J_0(\xi \rho), \quad (11)$$

and

$$\int_0^{2\pi} d\beta \int_0^{2\pi} d\beta_i e^{i\{\xi_i \rho_0 \cos(\beta_i - \phi_0) + \xi \rho \cos(\beta - \phi)\}} \cos m(\beta_i - \beta) \\ = (2\pi)^2 \cos m\pi \cos m(\phi_0 - \phi) J_m(\xi_i \rho_0) J_m(\xi \rho). \quad (12)$$

After some straightforward algebraic manipulation, the field scattered from a sphere in a layered medium takes the form

$$\Phi_s(\mathbf{r}, \mathbf{r}_0) = \frac{(2\pi)^2}{\pi k} \sum_{n=0}^{\infty} f(n) \\ \times \left\{ \int_0^{\infty} \left[ \Psi^+(z_0) P_n \left( -\frac{\gamma_i}{k} \right) + \Psi^-(z_0) P_n \left( \frac{\gamma_i}{k} \right) \right] J_0(\xi_i \rho_0) \xi_i d\xi_i \int_0^{\infty} \left[ \Psi^+(z) P_n \left( -\frac{\gamma}{k} \right) + \Psi^-(z) P_n \left( \frac{\gamma}{k} \right) \right] J_0(\xi \rho) \xi d\xi \right. \\ \left. + 2 \sum_{m=1}^n \frac{(n-m)!}{(n+m)!} \cos m(\phi - \phi_0 + \pi) \right. \\ \left. \times \left\{ \int_0^{\infty} \left[ \Psi^+(z_0) P_n^m \left( -\frac{\gamma_i}{k} \right) + \Psi^-(z_0) P_n^m \left( \frac{\gamma_i}{k} \right) \right] J_m(\xi_i \rho_0) \xi_i d\xi_i \int_0^{\infty} \left[ \Psi^+(z) P_n^m \left( -\frac{\gamma}{k} \right) + \Psi^-(z) P_n^m \left( \frac{\gamma}{k} \right) \right] J_m(\xi \rho) \xi d\xi \right\} \right\}. \quad (13)$$

This formula is particularly useful for computational purposes because it expresses the 3-D field scattered from a sphere solely in terms of 1-D wave number integrals. The fourfold reduction in the dimensionality of the general spectral transform of Eq. (3) is a consequence of the spherical symmetry of the object. As a matter of practicality, the integrals typically converge in shallow-water acoustic applications when the horizontal wave number magnitude reaches an upper limit that exceeds, but is well within an order of magnitude of,  $k$ , while the summations generally converge after roughly  $2ka$  terms are taken. It is noteworthy that the first term,  $n=0$ , of Eq. (13) is the general solution for an arbitrarily shaped compact object ( $\lambda \gg a$ ) in a waveguide.

To examine the ranges within which Eq. (13) is valid, it is useful to consider the field scattered from a sphere in free space

$$\Phi_s(\mathbf{r}) = - \sum_{n=0}^{\infty} i^n (2n+1) a_n h_n^{(1)}(kr) P_n(\cos \theta \cos \alpha_i) \\ + \sin \theta \sin \alpha_i \cos(\phi - \beta_i), \quad (14)$$

by an incident plane wave propagating in the direction  $(\alpha_i, \beta_i)$ . Since

$$h_n^{(1)}(kr) \approx (-i)^{n+1} \frac{e^{ikr}}{kr}, \quad (15)$$

for  $kr \gg 1$  and  $kr > n$ , the scattered field can be approximated by

$$\Phi_s(\mathbf{r}) \approx \frac{e^{ikr}}{kr} S(\theta, \phi; \alpha_i, \beta_i), \quad (16)$$

for  $kr \gg 1$  and  $kr > 2ka$ , or  $r > 2a$ , since satisfactory convergence typically occurs after  $2ka$  terms are taken in Eq. (14). This approximation, therefore, can be a good one very close to the sphere's surface. For practical applications, it is usually valid well within the object's nearfield since  $(2a)^2/\lambda$  thresholds onset of the far field. By similar reasoning, the Bessel functions in Eq. (13) can be approximated by their asymptotic forms for large arguments.

For objects in a shallow-water waveguide, however, neglect of multiple-scattering from the waveguide boundaries

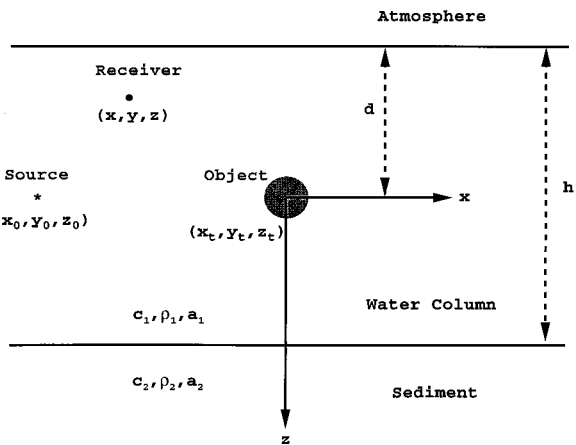


FIG. 2. Geometry of a spherical object in a Pekeris waveguide insonified by a point source. To be consistent with subsequent calculations, the point source and object centroid are shown at the center of the waveguide where  $h = 100$  m,  $d = 50$ , and the sphere radius is  $a = 10$  m.

will sometimes lead to more stringent limitations on the range within which Eq. (13) remains a valid approximation. For most practical applications in shallow-water acoustics, however, the effects of multiple-scattering between the object and waveguide boundaries are only expected to be significant over horizontal ranges within roughly two diameters of the object centroid. They are expected to be most pronounced when the object's diameter is on the order of the strata thickness, and negligible when the diameter is much less than the strata thickness. Examples of multiple scattering and errors introduced by neglecting it have been given in Refs. 17 and 2.

### III. SCATTERING FROM A SPHERICAL OBJECT IN A SHALLOW-WATER WAVEGUIDE

#### A. Pekeris waveguide

Equation (13) is used to numerically compute the field scattered from a spherical object in a shallow-water waveguide. For simplicity the waveguide is assumed to be Pekeris with water column sound speed  $c_1 = 1500$  m/s, density  $\rho_1 = 1000$  kg/m<sup>3</sup>, and attenuation  $a_1 = 3 \times 10^{-4}$  m<sup>-1</sup> overlaying a sediment half-space of sound speed  $c_2 = 1700$  m/s, density  $\rho_2 = 1900$  kg/m<sup>3</sup>, and attenuation  $a_2 = (0.1/\lambda)$  m<sup>-1</sup>. The waveguide geometry is shown in Fig. 2. Analytic expressions for the up- and down-going plane wave amplitudes of the incident field and medium Green's function are provided in the Appendix.

Both the point source, of strength 0 dB *re*: 1  $\mu$ Pa at 1 m, and sphere centroid are located in the middle of the water column so that  $d = h/2$  where  $h = 100$  m. The source, located at  $(x_0 = -4000$  m,  $y_0 = 0$ ,  $z_0 = 0)$ , is therefore separated from the sphere centroid by 4-km horizontal range. The homogenous sphere is assumed to have a radius of  $a = 10$  m and to satisfy pressure release boundary conditions at its surface. Computations are made at frequency  $f = 300$  Hz so that the number of wavelengths that fit across the sphere's circumference,  $ka$ , is roughly 12.6.

The results of the computations are shown in Figs. 3 and 4. To help understand their meaning, they are presented

along with a standard but crude sonar-equation approximation for the field scattered from an object in a waveguide

$$\Phi_s(\mathbf{r}) \approx \frac{4\pi}{k} G(\mathbf{r}|0)G(0|\mathbf{r}_0)S\left(\frac{\pi}{2}, \varphi; \frac{\pi}{2}, \phi_0 - \pi\right), \quad (17)$$

where the scattering function, which determines target strength and is plotted for the given object in Fig. 5, factors from transmission coefficients to and from the object. This type of approximation has been discussed by Ingenito.<sup>1</sup> It becomes valid in Eqs. (3) and (4) when propagation is effectively horizontal, so that  $\alpha_i \approx \alpha \approx \pi/2$ , and the incident and received fields are effectively planar, so that  $\beta_i \approx \phi_0 + \pi$  and  $\beta \approx \phi$ . It also becomes valid for compact objects ( $a \ll \lambda$ ) regardless of the waveguide's modal structure, as can be seen by taking *only* the first term,  $n = 0$ , of Eq. (13) as the general compact-object solution, noting that  $z_i$  must vanish for a point target at the origin and that the plane wave scattering function reduces to  $f(0)$  and so becomes independent of the incident and scattered angles. At 300 Hz, however, propagation in the waveguide of Figs. 2–4 is far from horizontal and the object is noncompact.

It is not surprising then that serious discrepancies arise between the sonar-equation approximation and the spectral formulation of Eq. (13). In particular, the sonar-equation approximation drastically overestimates the overall level of the scattered field, by tens of dB, as is evident in Fig. 3(a)–(b), where the scattered field is shown over a horizontal plane slicing through the center of the water column. This *absolute* error is *highly sensitive* to slight variations in the location of the source, target, and receiver, due to the complex interference structure within the waveguide. The sonar-equation approximation also significantly overestimates the level of the scattered field in the forward direction relative to other directions. But this error is *insensitive* to slight variations in source, target, or receiver locations because it is in *relative* level.

Besides the expected forward scatter beam of width  $\pi/(ka)$ , three other azimuthal beams of similar dimension are observed in Fig. 3(b). These fall within roughly two water column depths horizontal range of the object, between forward and backscatter directions. Since the beams are not observed in Fig. 5, they have no analogue in free-space scattering from an identical object. The beams apparently arise as interference from multiple images of the object. Since the beams are intimately related to the object's noncompactness, they are not present in the sonar-equation approximation. The 3-D nature of these beams can be explored by considering the range-depth plots of Fig. 4, where drastic azimuthal variations in the range–depth structure of the scattered field are observed in the vicinity of the object. While multiple images of the object are accounted for, as is consistent with waveguide propagation, multiple scattering between these images is neglected in the single-scatter formulation of Eqs. (3) and (4). The field structure within roughly two object diameters of the centroid, or roughly 40-m range, therefore may not be very accurate. But this has no effect on the noted beams which extend well beyond this range.

In the forward direction, Fig. 4(c), two vertical beams emerge from the object. The mean directions and relative

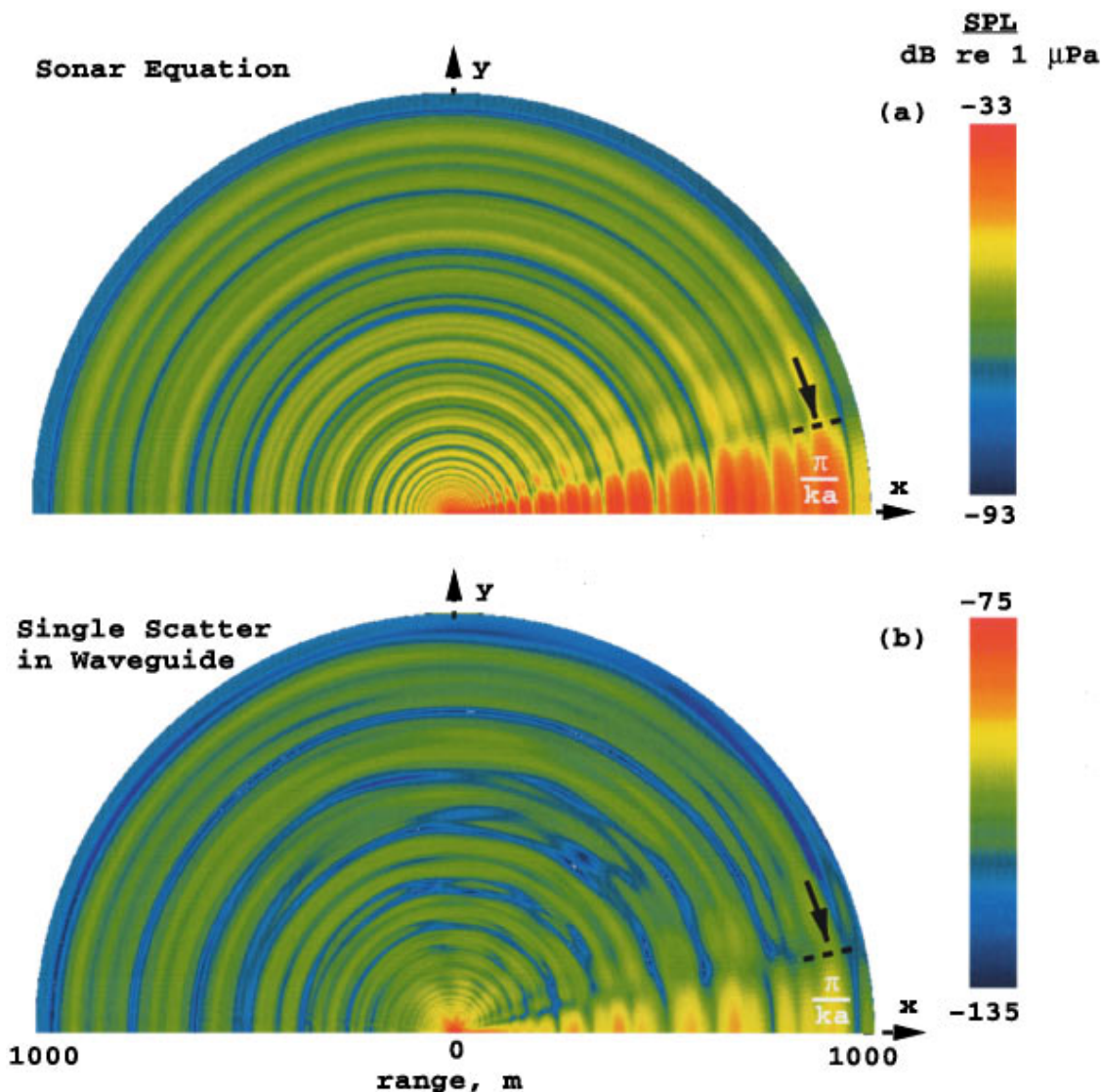


FIG. 3. Horizontal slice of the field scattered from a 10-m radius pressure release sphere, submerged in the middle of a 100-m-deep Pekeris waveguide, by a harmonic point source also in middle of the waveguide at  $(x_0 = -4000 \text{ m}, y_0 = 0, z_0 = 0)$  radiating at  $f = 300 \text{ Hz}$ . Image plane cuts through the object centroid placed in the middle of the waveguide. (a) For comparison, the sonar-equation approximation following Eq. (17) is shown for the noncompact object ( $ka = 12.6$ ). (b) Single-scatter calculation using Eq. (13).

intensities of these two beams roughly correspond to those of the equivalent up- and down-going plane waves for the most dominant discrete modes of the incident field. The forward scattered beamwidths can be interpreted as the convolution of this bimodal incident plane wave spectrum with the Poisson cone,<sup>2,12</sup> of angular width  $\pi/(ka)$ , for an individual plane wave.

### B. Implications for remote classification of general objects submerged in shallow water

While the range-depth field structure predicted by the sonar-equation approximation is in serious error in the vicinity of the object, it becomes better with increasing range. Apparently, as horizontal range increases, the bandwidth of the vertical angular spectrum decreases, by bottom transmission and attenuation, to the point that it is on the order of or less than  $\pi/(ka)$ . Beaming and interference effects arising from the object's noncompactness are then *no longer resolv-*

*able by vertical apertures* within the waveguide, and the range-depth structure converges to that of a monopole source placed at the object centroid, as is evident upon comparison of Fig. 4(a) with Fig. 4(b)–(d). The *full complexity* of scattering from a noncompact object in a multi-modal waveguide, however, is *maintained by the azimuthal structure* of the scattered field regardless of range since no boundaries are present to provide a similar reduction in bandwidth over azimuthal angle.

At ranges in great excess of the water column depth, therefore, classification of the object by a *single vertical aperture* would require *a priori* knowledge of the aspect of the object relative to the source and receiver, since *only the absolute level* of the field can be used to characterize the object. With an *azimuthal aperture*, on the other hand, classification can be made at such distant ranges merely by examining the normalized *spatial structure* of the received field.

The implication here is that multistatic observations of

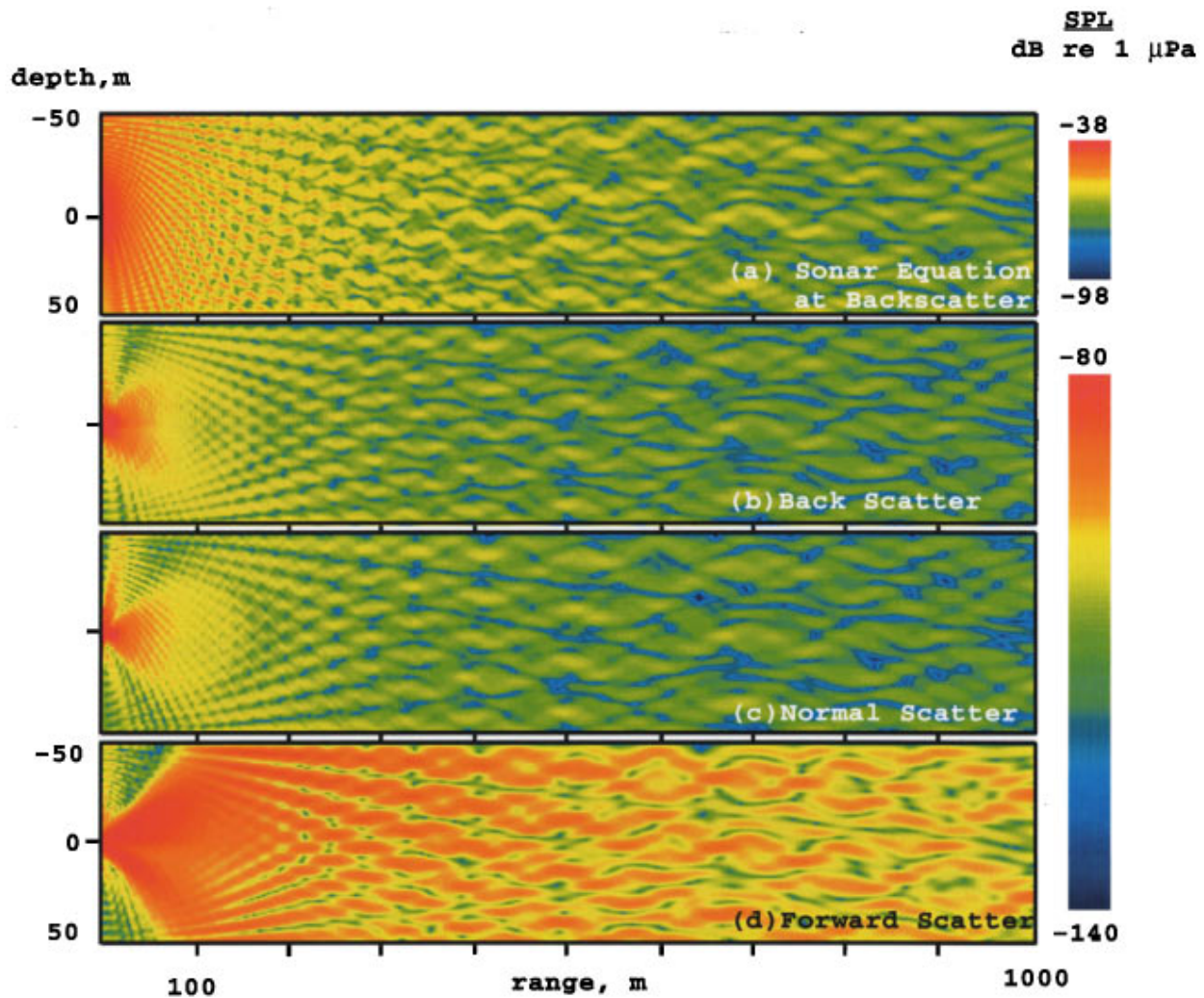


FIG. 4. Range-depth cross sections of the field scattered from a 10-m radius pressure release sphere, submerged in the middle of a 100-m-deep Pekeris waveguide, by a harmonic point source also in the middle of the waveguide at  $(x_0 = -4000 \text{ m}, y_0 = 0, z_0 = 0)$  radiating at  $f = 300 \text{ Hz}$ . (a) For comparison, the sonar-equation approximation of Eq. (17) is shown with levels corresponding to the backscatter azimuth. For the given noncompact object, Eq. (17) incorrectly yields range–depth structure that is invariant over azimuth and identical to point-source structure. To obtain the sonar-equation approximation at the forward scatter azimuth, uniformly augment the level by 24 dB over the entire Fig. 4(a). (b)–(d) Single-scatter calculation using Eq. (13) at azimuths corresponding to (b) backscatter, (c) normal scatter, and (d) forward scatter. Range increases along the negative  $x$  axis in (a) and (b), along the positive or negative  $y$  axis in (c), and along the positive  $x$  axis in (d). In single-scatter calculations, range–depth structure correctly shows drastic variation over azimuth in the vicinity of the noncompact object.

the scattered field, distributed over an azimuthal range greatly in excess of  $\pi/(ka)$ , will typically be necessary to classify an object submerged in a shallow-water waveguide at ranges exceeding the water column depth. By reciprocity, such multistatic observations may be made either by varying the relative azimuth of the source or receiver.

### C. Implications for measurement of the scattered field

In reality, source signals have finite time duration. In active sonar systems, time separation between the incident and scattered waveform arrivals is generally built-in to the operational geometry to insure that the incident field will not significantly overlap the scattered field at the receiver, except in the forward direction where no time separation is possible. Time separation of this kind is often essential for the scattered field to be measured by a single *omni-directional* sensor because while the incident field only suffers spreading

loss from the source, the scattered field suffers spreading loss from both the source to the object and from the object to the receiver. Given a *directional* sensor, with sufficient spatial aperture, however, the scattered field can be distinguished from the incident field even when there is no time separation by exploiting differences in propagation direction and field structure, as is done routinely in beamforming and matched field processing.

For the specific harmonic example described in Sec. III A, the total field, defined as the sum of the incident and scattered fields, has a sound pressure level that differs from the incident field by no more than a small fraction of a decibel over the regions shown in Figs. 3–4. In other words, relative to the incident field, the scattered field comprises an extremely small contribution to the total field amplitude. The reason for this can be understood better by analyzing the scattered field where it is strongest, namely in the two forward beams that appear in Fig. 4(d) within roughly one water

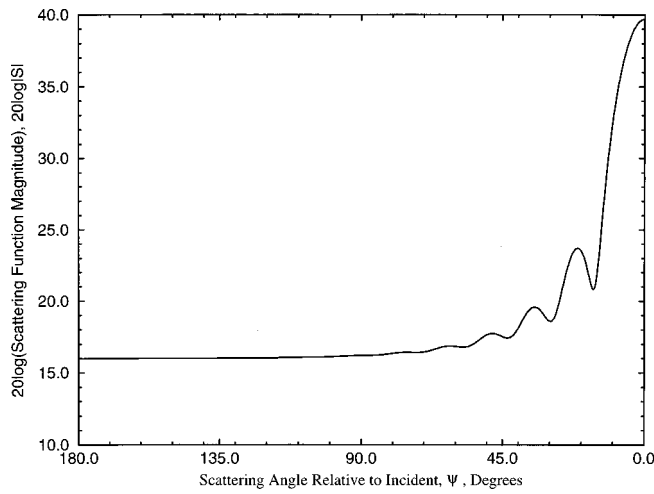


FIG. 5. The scattering function magnitude  $|S(\psi)|$  for a pressure-release sphere of  $ka=12.6$  is plotted as a function of the angle  $\psi$  between an incident plane wave from the direction  $(\theta_0, \phi_0)$  of a source and a plane wave scattered in the direction  $(\theta, \phi)$  of a receiver, where  $\cos \psi = \cos(\pi - \theta_0)\cos \theta + \sin(\pi - \theta_0)\sin \theta \cos(\phi - \phi_0 + \pi)$ , and forward scatter occurs at  $\psi=0$ . For example,  $\psi=\phi$  when  $\theta_0=\pi/2$ ,  $\phi_0=\pi$ , and  $\theta=\pi/2$ , as is relevant in Fig. 3.

column depth in range from the object. At any point in these beams, the *incident* field is the *convergence* of a *broad directional spectrum* of incident plane waves, in keeping with waveguide propagation from a distant point source. At the same point within these beams, however, the scattered field emanating from the object is in the process of *diverging*. Moreover, as discussed in Sec. III A, each beam corresponds to the forward scatter of only a *fraction* of the incident spectrum, due to directional filtering by the object, whereas the incident field is comprised of the *entire* incident spectrum, by definition.

While the present harmonic analysis can be extended to finite-time duration and broadband source signals by Fourier synthesis, without loss of generality, it is already approximately valid for *narrow-band* waveforms. For example, distinct narrow-band conditions can be given for the free-space scattering and waveguide propagation problems, each of which must be satisfied for the narrow-band approximation to be made in the waveguide scattering problem. In the former, the waveform's bandwidth about the carrier frequency must be much smaller than the ratio of the mean sound speed to the object diameter, so that the spatial extent of the signal pulse is much greater than that of the object. In the latter, the Green function from the source to the object, and similarly from the object to the receiver, must effectively be constant within the signal band. This latter condition typically requires the bandwidth to decrease as the bistatic range from source to object and from object to receiver increases.

#### IV. CONCLUSIONS

A spectral formulation for 3-D object scattering in a layered medium is described. The formulation is valid when the source and receiver are sufficiently far from the object that multiple scattering between the object and waveguide boundaries can be neglected and the scattered field can be expressed as a linear function of the object's plane wave

scattering function. Since these conditions are often satisfied in active sonar problems, especially those involving remote objects, and the formulation is relatively simple to implement, it is of practical value in a wide variety of ocean-acoustic applications.

An analytic expression is derived for the field scattered from a spherical object in a stratified medium. Since the expression is in terms of 1-D wave number integrals, it is computationally efficient to implement, allows detailed investigation of the scattered field in the vicinity of the object, and enables scattering of evanescent waves to be incorporated by analytic continuation.

Computations for a noncompact sphere illustrate the essential characteristics of 3-D object scattering in a shallow but multi-modal waveguide. For example, a significant decrease in the relative level of the scattered field in the forward direction, compared with free-space scattering, as well as a pronounced 3-D beaming effect in the vicinity of the sphere are discovered.

Another primary finding is that on vertical apertures, at sufficiently large ranges from the object, the structure of the scattered field converges to that of a monopole source placed at the object centroid. This convergence occurs when the bandwidth of the vertical angular spectrum decreases, by bottom transmission and attenuation, to the point that it is on the order of or less than  $\pi/(ka)$ . In this case only a constant scale factor is available to classify the object, given *a priori* knowledge of its aspect. As a result, multistatic observations of the scattered field, distributed over an azimuthal aperture greatly in excess of  $\pi/(ka)$ , will typically be necessary to classify an object submerged in a shallow-water waveguide at ranges exceeding the water column depth.

Finally, standard sonar equation analysis is found to be a highly unreliable method for estimating the level of the field scattered from noncompact objects submerged in shallow water.

#### APPENDIX

For a Pekeris waveguide of thickness  $h$  with object centroid at vertical distance  $d$  from the air-sea interface, as shown in Fig. 2, the plane wave coefficients for the incident field  $\Phi_i(\mathbf{r})$  are

$$\Psi^+(z_0) = \frac{1}{4\pi i \gamma_i} \left( \frac{e^{i\gamma_i(z_0+2d)} - e^{-i\gamma_i z_0}}{1 + R_i e^{i2\gamma_i h}} \right), \quad (\text{A1})$$

$$\Psi^-(z_0) = \frac{R_i e^{i2\gamma_i h}}{4\pi i \gamma_i} \left( \frac{e^{i\gamma_i z_0} - e^{-i\gamma_i(z_0+2d)}}{1 + R_i e^{i2\gamma_i h}} \right), \quad (\text{A2})$$

when  $h-d \geq z_i > z_0$ , and

$$\Psi^+(z_0) = \frac{1}{4\pi i \gamma_i} \left( \frac{e^{i\gamma_i(z_0+2d)} + R_i e^{i2\gamma_i h} e^{-i\gamma_i z_0}}{1 + R_i e^{i2\gamma_i h}} \right), \quad (\text{A3})$$

$$\Psi^-(z_0) = -\frac{1}{4\pi i \gamma_i} \left( \frac{e^{i\gamma_i z_0} + R_i e^{i2\gamma_i h} e^{-i\gamma_i(z_0+2d)}}{1 + R_i e^{i2\gamma_i h}} \right) \quad (\text{A4})$$

when  $z_0 > z_i \geq -d$ . These are in terms of the reflection coefficient between the water column and sediment

$$R_i = \frac{\rho_2 \gamma_i / \rho_1 v_i - 1}{\rho_2 \gamma_i / \rho_1 v_i + 1}, \quad (\text{A5})$$

where the vertical wave number in the sediment  $v_i$  is defined by  $k^2(z) = v_i^2 + \xi_i^2$ . Water column attenuation  $a_1$  is included by setting  $k(z) = \omega/c_1 + ia_1$ , where  $c_1$  is the sound speed in the water column. Sediment attenuation  $a_2$  is included by setting  $k(z) = \omega/c_2 + ia_2$ , where  $c_2$  is the sound speed in the sediment.

Conversely for the Green's function  $G(\mathbf{r}|\mathbf{r}_i)$ , the plane wave amplitudes are

$$\Psi^+(z) = \frac{1}{4\pi i \gamma} \left( \frac{e^{i\gamma_i(z+2d)} + R e^{i2\gamma h} e^{-i\gamma z}}{1 + R e^{i2\gamma h}} \right), \quad (\text{A6})$$

$$\Psi^-(z) = -\frac{1}{4\pi i \gamma} \left( \frac{e^{i\gamma z} + R e^{i2\gamma h} e^{-i\gamma(z+2d)}}{1 + R e^{i2\gamma h}} \right), \quad (\text{A7})$$

for  $h-d \geq z > z_i$ , and

$$\Psi^+(z) = \frac{1}{4\pi i \gamma} \left( \frac{e^{i\gamma(z+2d)} - e^{-i\gamma z}}{1 + R e^{i2\gamma h}} \right), \quad (\text{A8})$$

$$\Psi^-(z) = \frac{R e^{i2\gamma h}}{4\pi i \gamma} \left( \frac{e^{i\gamma z} - e^{-i\gamma(z+2d)}}{1 + R e^{i2\gamma h}} \right), \quad (\text{A9})$$

for  $z_i > z \geq -d$ .

<sup>1</sup>F. Ingenito, "Scattering from an object in a stratified medium," *J. Acoust. Soc. Am.* **82**, 2051–2059 (1987).

<sup>2</sup>N. C. Makris, F. Ingenito, and W. A. Kuperman, "Detection of a submerged object insonified by surface noise in an ocean waveguide," *J. Acoust. Soc. Am.* **96**, 1703–1724 (1994).

<sup>3</sup>N. C. Makris and D. H. Cato, "Acoustic tracking of non-vocalizing whales using the scattered field of vocalizing whales," in *Proceedings of the Australian Acoustical Society*, Sydney, Australia (1994).

<sup>4</sup>N. C. Makris, "Bistatic detection of underwater objects using directional surf noise as a source of opportunity," pp. A16-1–A16-7, in *ASW Surveillance Programs* (Office of Naval Research, Arlington, VA, 1996).

<sup>5</sup>While it may be the earliest reference on the general subject of scattering from an object in a waveguide, this paper is not directly relevant to ocean-acoustics since its treatment is restricted to cylindrical waveguides. A. Bostrom, "The  $T$ -matrix method for scattering by an obstacle in a waveguide," in *Acoustic, Electromagnetic and Elastic Wave Scattering*, edited by V. V. Varadin and V. K. Varadin (Pergamon, New York, 1980), pp. 221–224.

<sup>6</sup>R. H. Hackman and G. S. Sammelmann, "Acoustic scattering in an inhomogeneous waveguide: Theory," *J. Acoust. Soc. Am.* **80**, 1447–1458 (1986).

<sup>7</sup>R. H. Hackman and G. S. Sammelmann, "Multiple scattering analysis for a target in an ocean waveguide," *J. Acoust. Soc. Am.* **84**, 1813–1825 (1988).

<sup>8</sup>M. D. Collins and M. F. Werby, "A parabolic equation model for scattering in the ocean," *J. Acoust. Soc. Am.* **85**, 1895–1902 (1989).

<sup>9</sup>J. S. Perkins, W. A. Kuperman, K. D. Heaney, and G. T. Murphy, "Scattering from an object in a three-dimensional ocean," *Proceedings of the 20th Annual International Meeting of the Technical Cooperation Subgroup, Subgroup G, Technical Panel 9*, October 1991.

<sup>10</sup>J. S. Perkins, W. A. Kuperman, L. E. Tinker, and G. T. Murphy, "Active matched field processing," *J. Acoust. Soc. Am.* **91**, 2366 (1992).

<sup>11</sup>The following reference presents a single-scatter modal approach similar to Ingenito's except that it employs  $T$ -matrix techniques: G. V. Norton and M. F. Werby, "A numerical technique to describe acoustical scattering and propagation from an object in a waveguide," *J. Appl. Phys.* **70**, 4104–4112 (1991).

<sup>12</sup>J. J. Bowman, T. B. A. Senior, and P. L. E. Uslenghi, Eds., *Electromagnetic and Acoustic Scattering by Simple Shapes* (North-Holland, Amsterdam, 1969). While the entire book is relevant, see Chap. 10 for application to spheres.

<sup>13</sup>R. J. Urlick, *Principles of Sound in the Sea* (McGraw-Hill, New York, 1983), pp. 306–327.

<sup>14</sup>K. Aki and P. G. Richards, *Quantitative Seismology: Theory and Methods* (Freeman, New York, 1980), pp. 273–286.

<sup>15</sup>F. B. Jensen, W. A. Kuperman, M. B. Porter, and H. Schmidt, *Computational Ocean Acoustics* (AIP Press, New York, 1994), pp. 203–270.

<sup>16</sup>P. M. Morse and K. U. Ingard, *Theoretical Acoustics* (Princeton U. P., Princeton, NJ, 1986), pp. 418–436.

<sup>17</sup>J. A. Fawcett, "Scattering from an elastic cylinder buried beneath a rough water/sediment interface," in *High Frequency Acoustics in Shallow Water* (NATO SACLANT Undersea Research Centre, La Spezia, Italy, 1997), pp. 147–154.